Weather and Climate Extremes 33 (2021) 100337

Contents lists available at ScienceDirect

Weather and Climate Extremes

journal homepage: www.elsevier.com/locate/wace

European extreme precipitation: The effects of spatio-temporal resolution of the data

Mostafa E. Hamouda [a,b,c,*], Claudia Pasquero [a,d]

[a] Department of Earth and Environmental Sciences, Universitá di Milano - Bicocca, Milan, Italy
[b] Astronomy and Meteorology Department, Faculty of Science, Cairo University, Cairo, Egypt
[c] Osservatorio Geofisico Sperimentale, Trieste, Italy
[d] Istituto di Scienze dell'Atmosfera e del Clima, Consiglio Nazionale delle Ricerche, Turin, Italy

ARTICLE INFO

Keywords:
Extreme precipitation trends
ERA reanalysis
High resolution
Convection permitting model WRF

ABSTRACT

European wintertime precipitation is known to be skilfully estimated in reanalysis data and model simulations since it is highly correlated with large scale, low frequency modes of variability, namely the North Atlantic Oscillation (NAO). Since the NAO is mainly a wintertime mode of variability, the skill of estimating precipitation becomes more limited in other seasons, most importantly in summer, when precipitation is mainly a result of mesoscale convection. In this study, we use the Weather Research and Forecast (WRF) model, to show the added value of using a high resolution, convection-permitting model to estimate precipitation extremes. The results show that WRF succeeds to correct the failure of ERA-Interim reanalysis to capture the positive trends over the last decades of European extreme precipitation in summer and transition seasons, that are indicated by observational data (E-OBS) and previous literature. Partial improvements are evident using ERA5 reanalysis, specifically in Spring and in Autumn. In winter, changes in European extreme precipitation over the last decades are dominated by variations in the NAO index, and are well reproduced both in reanalysis data and in the high resolution WRF downscaling.

1. Introduction

One of the most discussed effects of the current climate crisis is the change in the occurrence of extreme precipitation (Trenberth, 2011; Trenberth and Josey, 2007). Considering the rarity and the spatial heterogeneity of the events (Myhre et al., 2019), the determination of the existence of statistically significant trends is very challenging. A very large number of multidecadal time series is necessary to address the issue. Nevertheless, in the scientific community there is a growing consensus on the fact that there are more regions in which heavy precipitation is increasing than decreasing (IPCC, 2013; Papalexiou and Montanari, 2019; Seneviratne et al., 2012). The use of models and reanalysis data to support the observed trends is limited by their relatively low spatial resolution, especially considering that long simulations are required.

In some cases, observations have shown that heavy precipitation is correlated with large scale variability patterns, a link that is also well represented in models. For example, the changing frequency of atmospheric blocking is known to influence precipitation and temperature extreme variability over Europe (Sillmann and Croci-Maspoli, 2009; Buehler et al., 2011). Similarly, the trends observed in the occurrence of extreme North Atlantic cyclones impact heavy precipitation events in Europe (Wang et al., 2006; Raible, 2007).

Another important link that has been investigated in several studies is the one relating European precipitation to the North Atlantic Oscillation (NAO) (Hurrell, 1995; Walker and Bliss, 1932; Thompson and Wallace, 1998; Deser, 2000; Totz et al., 2017; Guérémy et al., 2012). The NAO is an alternation of high and low pressure anomalies between Icelandic and Azores pressure centers. A positive NAO phase is associated with low pressure anomalies in the Icelandic pressure center, and high pressure anomalies in the Azores pressure center. It deflects the Atlantic storm-track Northward, resulting in wet conditions over Northern Europe and dry conditions over Southern Europe. The opposite happens during the negative NAO phase. Previous literature has shown that both mean precipitation and the occurrence of extreme precipitation events in Europe during winter are influenced by the phase of the NAO (Scaife et al., 2008; Cohen et al., 2014; Casanueva et al., 2014). Considering that the NAO is well reproduced in reanalysis products, this relationship results in a relatively good skill of reanalysis to reproduce statistical properties of winter mean and extreme precipitation.

* Corresponding author at: Department of Earth and Environmental Sciences, Universitá di Milano - Bicocca, Milan, Italy.
E-mail address: m.hamouda@campus.unimib.it (M.E. Hamouda).

https://doi.org/10.1016/j.wace.2021.100337
Received 3 December 2020; Received in revised form 4 June 2021; Accepted 6 June 2021
Available online 11 June 2021

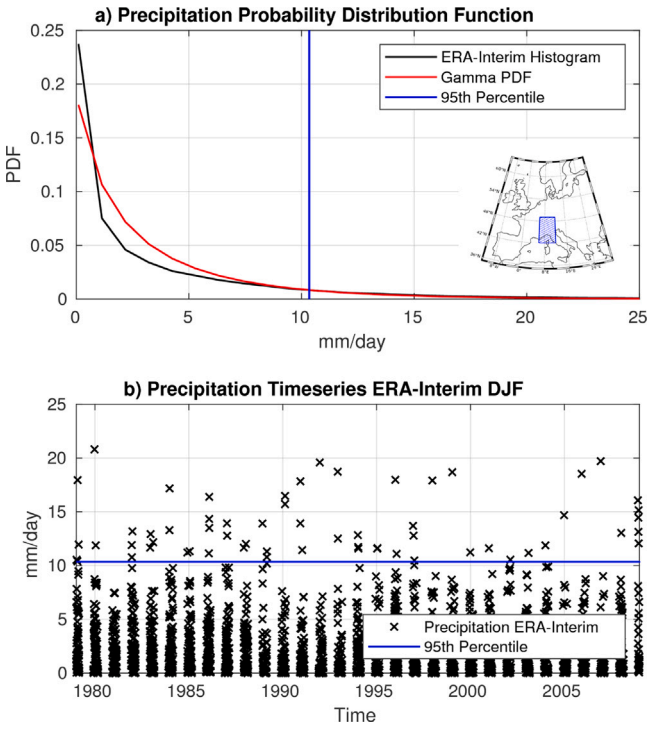

Fig. 1. (a) An example of the probability distribution function of the observed precipitation data of ERA-Interim reanalysis in winter season (DJF) for the region (9°E ± 3°, 45°N ± 3°, hatched in the map) (black), and the corresponding Gamma probability distribution function (red), with the 95th percentile threshold marked in (blue). b) Daily timeseries of wintertime ERA-Interim precipitation that is used to obtain the distribution function in (a), with the 95th percentile threshold marked by the blue line. (For interpretation of the references to color in this figure legend, the reader is referred to the web version of this article.)

The skill of models to reproduce the statistical properties of seasonal precipitation becomes significantly lower in the other seasons, most importantly in summer (Casanueva et al., 2014), when rainfall is partly associated with localized convection. A good representation of the convective scales requires the use of a high resolution, convection-permitting model, an approach that has been adopted in many studies (e.g. Schär et al., 2016; Leutwyler et al., 2017; Ban et al., 2015, 2020), as model physics and parameterizations play an important role in precipitation downscaling (Dereczynski et al., 2020), especially in complex orography regions (Giorgi et al., 2016). For example, it has been shown that summertime precipitation is highly underestimated over the UK using ERA-Interim reanalysis data (de Leeuw et al., 2015), and in Europe using CMIP5 models (Huang et al., 2017). ERA-Interim is known to have lower frequencies of extreme precipitation events due to its low spatial resolution (Skok et al., 2015), and summer extreme precipitation trends in Europe are also characterized by spatial variability that can have opposite signs in close regions (Zolina et al., 2005, 2008). For these reasons, the use of high resolution, convection-permitting models is a promising approach to have an added value for a better quantification of precipitation.

In this study, we compare heavy precipitation statistics and trends from observations, reanalysis, and high resolution dynamically downscaled data over a period of 30 years. Using different spatial and temporal resolution of the data, we assess their role in causing climatological changes to heavy precipitation.

In Section 2, we introduce data and methods, and in Section 3 we present and discuss the results. Discussion and summary are in Section 4

2. Data and methods

2.1. Data

The daily observational dataset is obtained from the EU-FP6 project UERRA (https://www.uerra.eu) and the Copernicus Climate Change Service, named E-OBS. It is constructed through a conditional simulation procedure interpolating station-derived meteorological observations, and comes as an ensemble dataset available on a 0.1 and 0.25 degree regular grid starting from 1950. In this study, the 0.1 degree ensemble is used from the period 1979 to 2008 which is the period that overlaps with the high resolution WRF simulations. More details about E-OBS construction are found in (Cornes et al., 2018).

In this study, E-OBS gridded dataset is taken as the reference "truth". However, it is noted that gridded observation datasets also have some limitations that arise from interpolation and homogenization techniques (Hofstra et al., 2009; Frei and Schär, 1998). For example, over complex terrain like the Alpine region, precipitation is underestimated by up to 40% with respect to rain gauge dataset (Frei and Schär, 1998; Isotta et al., 2014).

Reanalysis data are obtained from the European Centre for Medium-Range Weather Forecasts (ECMWF) ERA-Interim (Dee et al., 2011) for precipitation and sea level pressure, in the period from 1979 to 2008. The spatial resolution is about 80 km. The most recent reanalysis data ERA5 is also used, for the same period, with spatial resolution of about 31 km (Hersbach et al., 2020).

For the high resolution dynamical downscaling of reanalysis data, we use the output of the simulation run by Institute of Atmospheric Sciences and Climate — CNR using the Weather Research and Forecasting (WRF) model. The simulation is run over the Euro-Cordex domain, forced by ERA-Interim reanalysis from 1979 to 2008. The output has been recorded at 3-hourly temporal resolution. The microphysics is treated according to (Thompson et al., 2004). The grid spacing is 0.037° (about 4 km) in an inner domain, two-way nested into an external domain with 0.11° grid spacing and directly forced by ERA-Interim at the boundaries. In this convection permitting simulation, no convective parameterization scheme is used. More details on the WRF dynamical downscaling can be found in Pieri et al. (2015).

The WRF simulation had previously been validated by comparing precipitation climatology with various observational data such as E-OBS, CRU and GPCC (Pieri et al., 2015). It was found that WRF 4-km simulation has a lower bias with respect to E-OBS data, compared with ERA-Interim reanalysis, specifically in the summer season JJA. Over the European domain, the percentage differences of WRF 4-km to E-OBS is 17%, while it is 21% for ERA-Interim to E-OBS.

In general, WRF 4-km simulation tends to perform exceptionally well in summer (3% with respect to HISTALP in the Great Alpine Region (GAR) and 17% with respect to E-OBS). Percentage differences rise to 34% with respect to E-OBS in winter season. More details about the simulations and the validation are found in Pieri et al. (2015).

2.2. Methods

The North Atlantic Oscillation is defined in Hurrell et al. (2003) by calculating the leading mode of the Empirical Orthogonal Function (EOF) for sea level pressure anomalies obtained from ERA-Interim reanalysis, for the domain (90° W–40° E, 20° N–80° N). Monthly data of DJF, JJA, MAM, and SON are considered to calculate the leading mode of the season. The linear trend of the period from 1979 to 2008 is removed, and the dataset is weighted by the square root of cosine of latitude (North et al., 1982), then the covariance matrix is computed. It is worth noting that the leading EOF pattern (here named NAO regardless of the period of the year in which it is computed) looks different in different seasons. While typical wintertime NAO pattern has two centers of action over Iceland and the Azores, summer NAO is characterized by a pattern that is shifted northwards with a slight

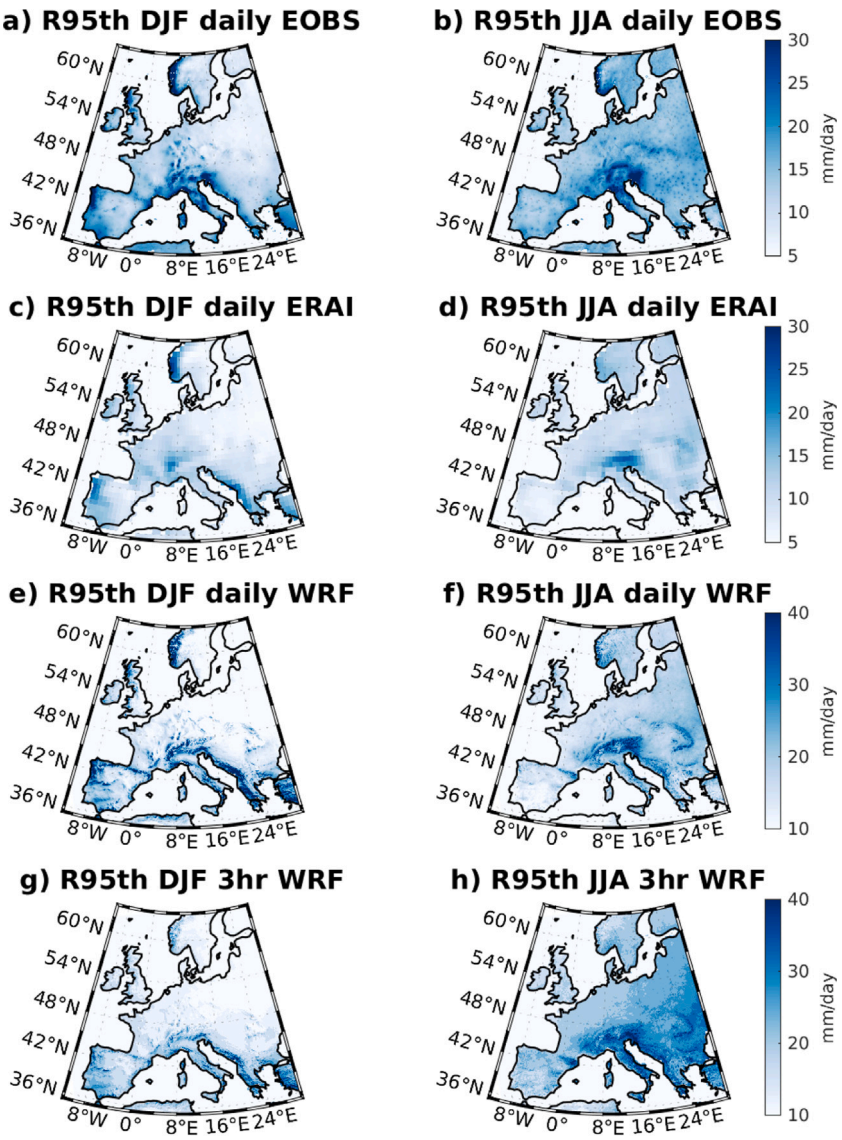

Fig. 2. The value of the 95th percentile of winter (left) and summer (right) precipitation using daily E-OBS (1st row), daily ERA-Interim reanalysis (2nd row), daily WRF downscaling (3rd row) and 3-hourly WRF downscaling (4th row) for the period from 1979 to 2008. (Unit: mm/day).

anticlockwise rotation of the axis of the maximum pressure gradient, and a significantly weaker Icelandic center of action (Folland et al., 2009; Bladé et al., 2011).

To estimate the 95th percentile of precipitation at each grid point, we use the procedure described in Husak et al. (2007) and Zolina et al. (2009). First, a distribution function is obtained using the whole (daily or three hourly) time series. We then fit a gamma distribution to the distribution function using shape parameter α and scale parameter β. To obtain α and β, let x be precipitation time series with length n_p:

$$A = \ln(\bar{x}) - \frac{\sum_i^{n_p} \ln(x_i)}{n_p}$$

$$\alpha = \frac{1}{4A}(1 + \sqrt{1 + \frac{4A}{3}})$$

$$\beta = \frac{\bar{x}}{\alpha}$$

Once the Gamma distribution is defined at each grid point, the corresponding 95th percentile threshold is obtained from the Gamma Cumulative Distribution Function. A sample of fitting Gamma probability distribution function to the probability distribution of observed precipitation data from ERA-Interim is shown in Fig. 1. The figure shows the probability distribution function for the region ($9°E \pm 3°, 45°N \pm 3°$) and the fitted Gamma distribution, which becomes more accurate when representing more extreme values of precipitation.

The interannual variability of extreme precipitation is then estimated following the procedure described in Papalexiou and Montanari (2019): we record the top 2.5% most extreme precipitation events over the 30 years of study. Then, a monthly time series of frequency of occurrence and accumulated intensity of extreme precipitation is obtained. The effects of the choice of the percentile of events studied was tested using 1.25%, 2.5%, 5%, and has no substantial influence on the conclusions.

To examine the effect of grid resolution on extreme precipitation trends, WRF 4-km simulation is also upscaled to match ERA-Interim grid resolution. Using First-order Conservative Remapping (Jones, 1999), WRF 4 km curvilinear grid was remapped to ERA-Interim longitude–latitude grid with a resolution of 80 km.

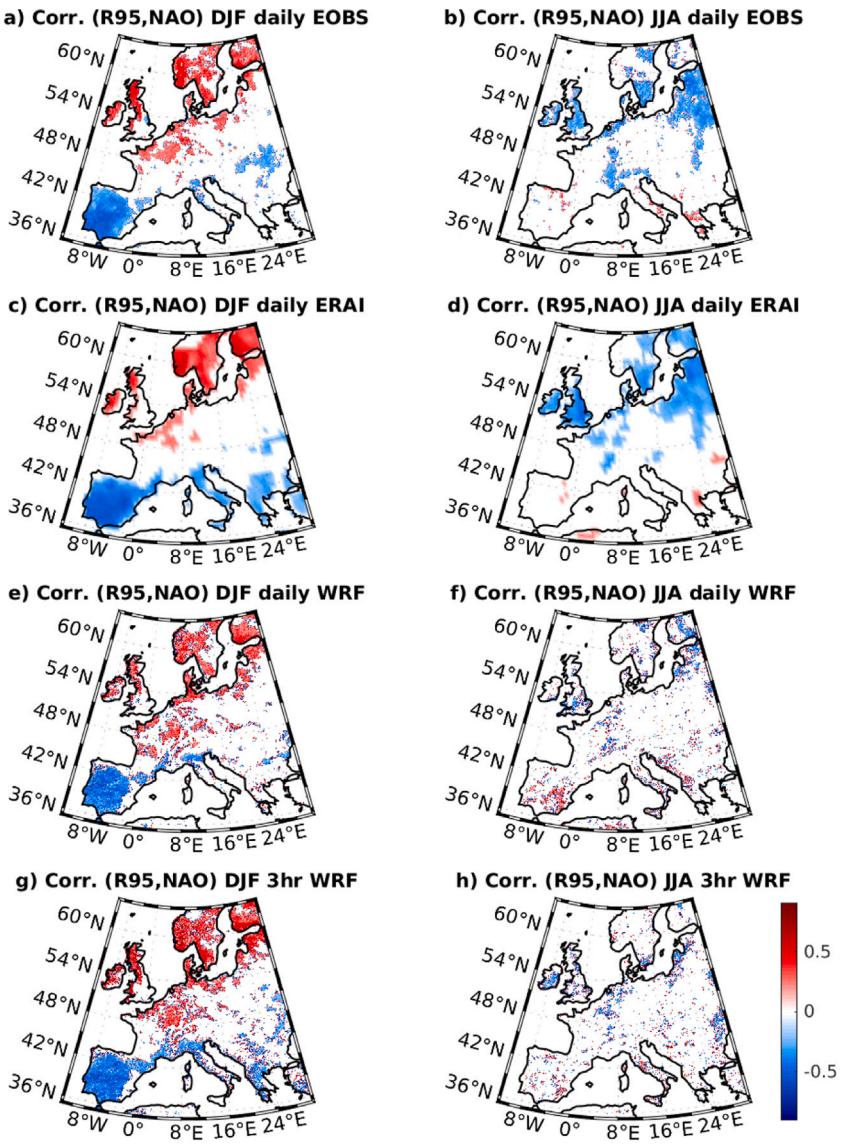

Fig. 3. Temporal correlation coefficient of monthly accumulated precipitation that exceeds the 95th percentile with NAO PC index in winter (left) and in summer (right) for daily E-OBS (1st row), daily ERA-Interim reanalysis (2nd row), daily WRF downscaling (3rd row) and 3-hourly WRF downscaling (4th row). Only statistically significant correlation ($p < 0.05$) is shown.

3. Results and discussion

3.1. Extreme precipitation threshold

The extreme precipitation threshold is defined as mentioned in Section 2.2 by fitting a Gamma distribution function to precipitation distribution function at each location, and identifying the corresponding 95th percentile value of the Gamma distribution.

Fig. 2 shows maps of the 95th percentile threshold of winter and summer precipitation for E-OBS, ERA-Interim reanalysis and its high resolution dynamical downscaling using WRF for daily and 3-hourly time scales. Spring and winter 95th percentile thresholds are shown in supplementary material, Figure S7.

The figures show that the patterns of the 95th percentile are in good agreement in the different seasons for the four datasets, where higher extreme thresholds follow coastlines and complex terrain regions. The high resolution data accommodates more detailed structures of extreme thresholds (Fig. 2e,f,g,h), particularly in regions with complex terrain (i.e. the Great Alpine Region). The different amplitudes of the 95th percentile between low resolution reanalysis and higher resolution E-OBS and WRF is owed to the spatial averaging in the low resolution grid box in ERA-Interim. Therefore, as expected, the high resolution downscaling is crucial for an accurate definition of the extreme precipitation at a given location.

The differences between the daily and 3-hourly accumulated precipitation in high resolution WRF output have a seasonal pattern: the 95% threshold is typically larger for daily values, except for the summer season. This can be rationalized as short-duration summer precipitation is typically a result of intense convective events. Consistent with Hodnebrog et al. (2019), sub-daily extreme precipitation pattern differs from that of the daily pattern, in which higher extreme value is indicated in the 3-hourly WRF simulation. This can be seen by comparing Figs. 2(f,h), where 3-hourly summer precipitation has generally a higher threshold than that of the daily.

3.2. Large scale synoptic variability

Many studies show how the North Atlantic Oscillation drives wintertime mean precipitation in Europe (e.g. Hurrell, 1995; Hurrell et al.,

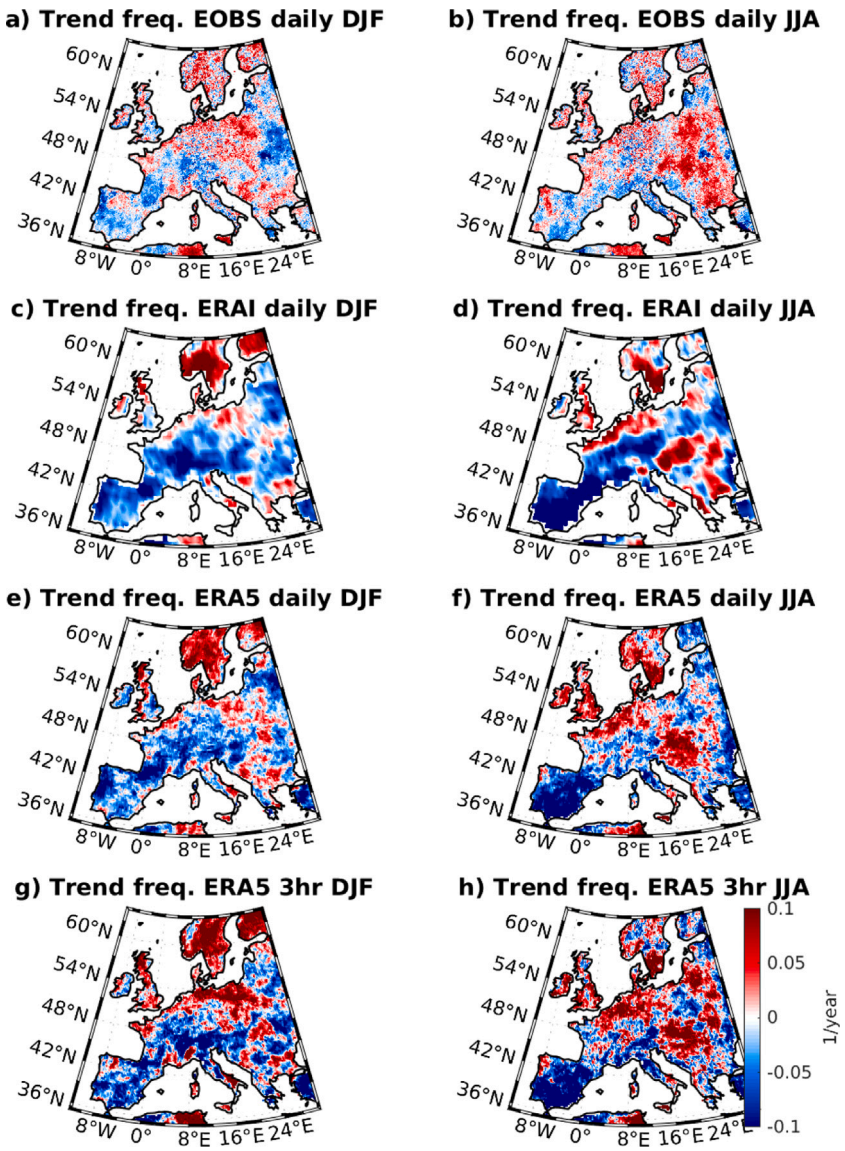

Fig. 4. Seasonal trends of extreme precipitation event frequency for daily E-OBS (1st row), daily ERA-Interim reanalysis (2nd row), daily ERA5 reanalysis (3rd row) and 3-hourly ERA5 (4th row). Unit: (1/year).

2003). Here, we show that not only mean rainfall is correlated with NAO, but also extreme precipitation are affected by the NAO phase (consistent with Casanueva et al., 2014). Fig. 3 shows the temporal correlation of the monthly accumulated precipitation exceeding the 95th percentile (shown in Fig. 2) with the NAO index, for winter and summer. Only significant correlations (p-value <0.05) are shown. For wintertime extreme precipitation, the figure shows the well known dipole-like correlation, in which extreme precipitation over northern Europe is correlated to NAO, while extreme precipitation over southern Europe is anti-correlated to NAO. As the leading mode of variability over the North Atlantic European sector in summer (here called summer NAO) is different from the winter NAO pattern, the correlation pattern between the summer NAO and extreme precipitation also differs compared to the winter pattern. Here we find anti-correlation signals over limited areas in northern Europe and unlike in Casanueva et al. (2014) and Bladé et al. (2011) no correlation between the summer NAO and extreme precipitation in southern Europe.

The temporal and spatial high resolutions are also examined using 4 km spatial resolution, daily and 3-hourly temporal resolution. Further positive correlation signal between the NAO and extreme precipitation in DJF appears over the Great Alpine Region in WRF 4 km simulation as in Fig. 3(e,g), a signal that is not evident in ERA-Interim reanalysis. By comparing the 3-hourly WRF simulations in figures (S2) for the transition seasons (SON and MAM), negative correlation of the short-lived extreme precipitation events with the NAO become significant for wider regions over Europe.

3.3. Seasonal trends of extreme precipitation

According to the Clausius–Clapeyron relation, when global temperature increases, the air can hold more moisture. More moisture means more frequent and intense extreme precipitation, as more latent heat released during condensation further increases the buoyancy of the air, favoring further upward motion and thus more condensation. This is concluded by some studies (e.g. Fischer and Knutti, 2016; Zolina et al., 2008; Papalexiou and Montanari, 2019), where rain gauges data and models show that the trend of extreme precipitation is positive in many locations, in correspondence to the warmer climate of the last decades. Here, we follow a similar analysis as in Papalexiou and Montanari (2019), by recording the top 2.5% most extreme precipitation events,

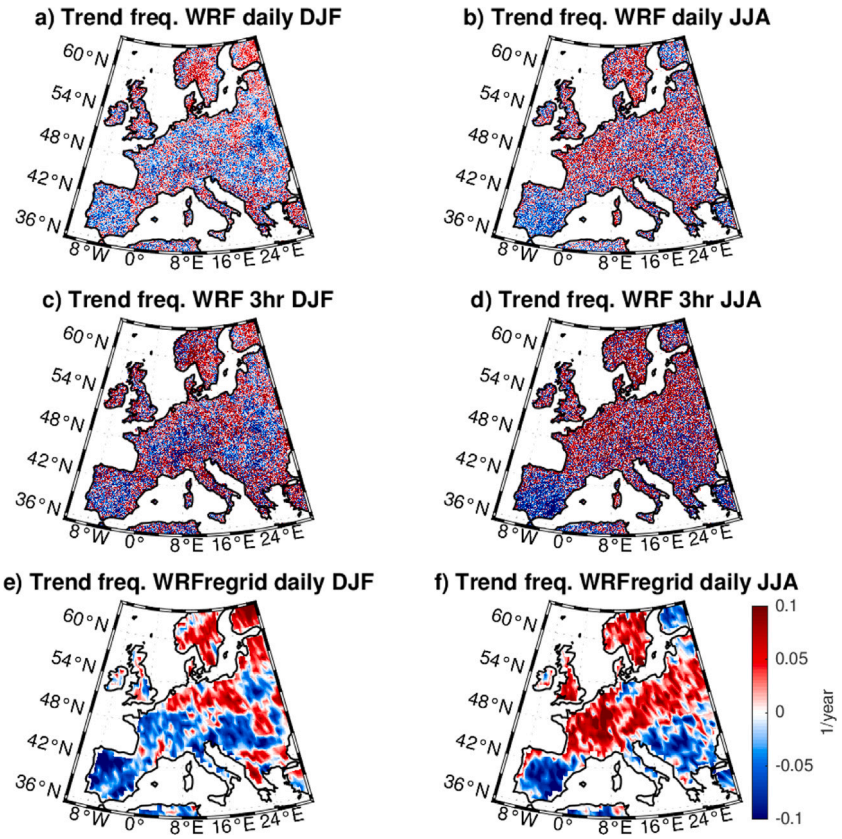

Fig. 5. Similar to Fig. 4, except for WRF daily data (1st row), WRF 3-hourly data (2nd row) and daily WRF data regridded to ERA-Interim resolution (3rd row).

then calculating the linear trend of extreme precipitation intensity and frequency of occurrence as detailed in Section 2.2.

Figs. 4, 5, S3, S4 show seasonal trends of extreme precipitation frequency of occurrence for daily E-OBS, daily ERA-Interim, daily and 3-hourly ERA-5 and WRF. Similarly, Figs. 6, 7, S5, S6 show seasonal trends of extreme precipitation intensity.

For wintertime, left column of Figs. 4–7 show mostly positive trends over Northern Europe, and generally negative trends over Southern Europe, an aspect that is common for all datasets, except for the 3-hourly WRF experiment, in which positive trends dominate in most of the domain.

The characteristic positive/negative dipole of daily precipitation trends for north/south Europe can be explained by the variability of NAO over the studied period (Scaife et al., 2008; Goodess and Jones, 2002; Pinto and Raible, 2012; Santos et al., 2018). As the NAO trend in the 1979–2008 period is positive, extreme precipitation increases in northern Europe, and drier conditions prevail over southern Europe. This wintertime characteristic dipole is summarized in Fig. 8. The figure shows the ratio of the count of grid points with positive trends to the count of grid points with negative trends, divided for Northern and Southern Europe. The separation latitude is taken at 49°N, which marks the change of the sign of precipitation correlation with winter NAO index in Fig. 3.

For summer and transition seasons, some agreement in the patterns between E-OBS, ERAI, ERA5, and WRF daily are evident (right column of Figs. 4–7). In summer, the Mediterranean Sea is considered an important source of moisture feeding extreme precipitation over central Europe (Hofstätter and Chimani, 2012; Messmer et al., 2015; James et al., 2004; Stohl and James, 2005; Krug et al., 2021), a source that is driven by the so-called Vb cyclone track, which is characterized by upper level strong south-westerly wind from the Mediterranean driving surface low pressure systems toward central Europe (van Bebber, 1891). In spite of this large scale control of summer precipitation, that should be well captured by reanalysis data, ERA-Interim and ERA5 fail to show positive trends of extreme precipitation over central Europe based on E-OBS (Figs. 4, 6)(d,f). The dynamical downscaling obtained in the WRF 4 km run succeeds to correct these trends (Figs. 5, 7(b,f)) and resemble the trends identified in E-OBS (Figs. 4, 6a). This result emphasizes the importance of resolving convective precipitation using high resolution models (Giorgi et al., 2016).

Extreme precipitation variability in non-winter seasons can be discussed in light of the warming Mediterranean Sea. This warming reduces baroclinicity, most importantly over the western Mediterranean region (Raible et al., 2009). Cyclonic activity tends to be suppressed, explaining the negative extreme precipitation trends over southwestern Europe (left column of Figs. 4–7). Moreover, the warmer sea has also been shown to cause enhanced precipitation over the Adriatic region, reducing moisture transport by Vb-cyclones to the eastern flanks of the Alps and central Europe (Messmer et al., 2016), where indeed negative extreme precipitation trends are observed.

The vast majority of the individual extreme precipitation time series does not have a statistically significant trend at the 95% confidence level (computed using Mann–Kendall test), as it can be expected given the very large interannual variability in the occurrence of extreme precipitation events. Nevertheless, it is still interesting to analyze them. In fact, in the null hypothesis of stationarity, we expect uncorrelated time series to present a similar number of positive and negative trends. A preferential occurrence of positive (or negative) trends thus allows us to reject the null hypothesis of stationarity. We computed the ratio of the count of positive to the count of negative trends over the domains as shown in Figs. 4–7 for extreme precipitation frequency and intensity (Fig. 9). A ratio higher than 1 means that there are more positive trends in the frequency of occurrence than negative ones. The opposite applies for ratios less than 1. As the number of degrees of freedom to compute

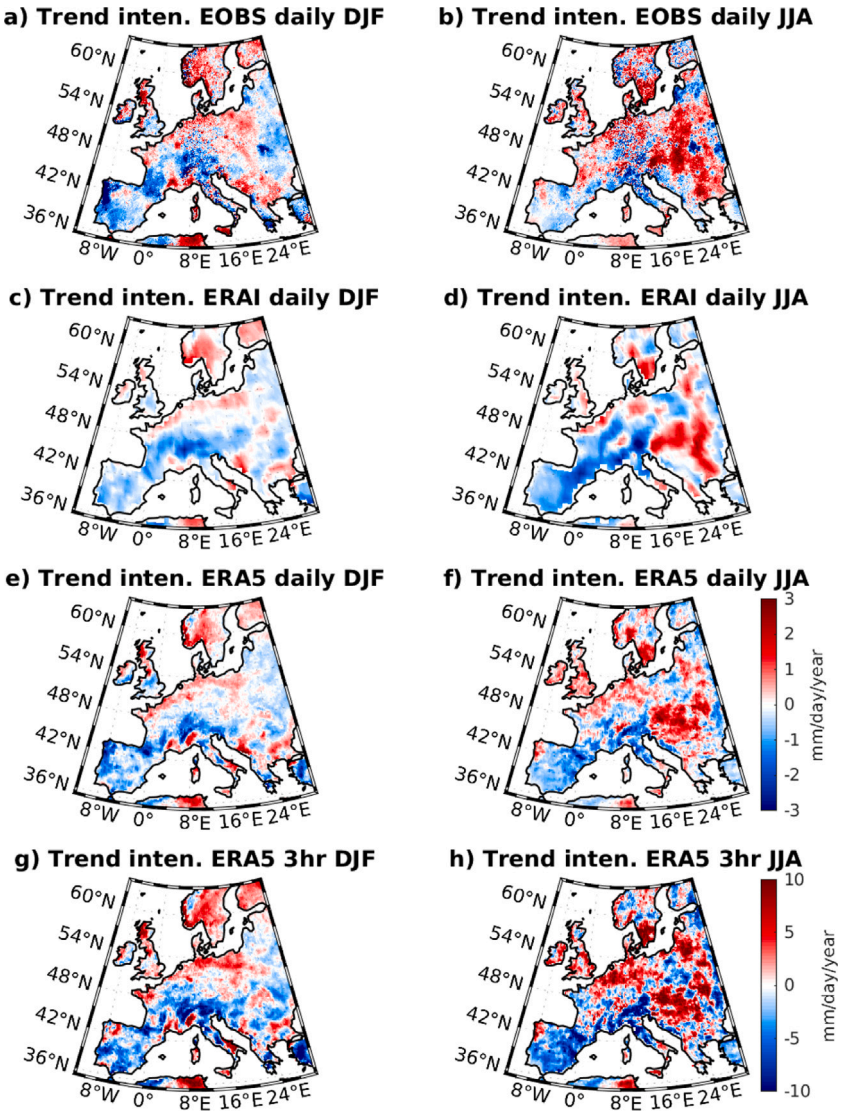

Fig. 6. Seasonal trends of extreme precipitation intensity for daily E-OBS (1st row), daily ERA-Interim reanalysis (2nd row), daily ERA5 reanalysis (3rd row) and 3-hourly ERA5 (4th row). Unit: (mm/day/year).

the ratio increases, the ratio should approach one in the null hypothesis of stationarity. The number of degrees of freedom in the system is not easily determined, but it is certainly much smaller than the number of grid points, because storms and large scale environmental conditions generate spatial correlations. In this study, we arbitrarily used 500 as the number of degrees of freedom, while the number of grid points was between O(10^3) and O(10^5), depending on the dataset used. E-OBS data indicate a ratio smaller than one for DJF and larger than one for all other seasons.

Wintertime extreme precipitation, as it has already been discussed, mainly reflects a dynamical change in the large scale atmospheric circulation associated to the NAO phase. The fact that the locations in which extremes decrease are more than the locations in which they increase can be linked to the fact that a large region in Europe has precipitation which are anti-correlated with NAO. Extreme precipitation in the rest of the year shows an overall increasing trend both in the frequency of occurrence and in their intensity (ratio larger than one) in the E-OBS dataset, suggesting that the overall increase expected in response to a warming world could be responsible for the observed signal over Europe.

Fig. 9 shows that ERA-Interim and ERA5 fail to capture the increasing frequency and intensity of extreme precipitation in summer and transition seasons, while they succeed in representing extreme precipitation changes in winter. This latter result is consistent with its link to NAO variability, that is well represented in reanalysis products. An improvement in using ERA5 with respect to ERA-Interim is evident in SON for frequency trends, and in MAM and SON for intensity trends. This could be due to the improved convective parameterization in ERA5 (Hersbach et al., 2020).

Higher temporal and spatial resolutions from WRF dynamical downscaling simulations show more consistent ratios with respect to gridded observation data (E-OBS), for which the ratio of the number of positive to negative trends for non-winter seasons is captured. During fall, however, high resolution WRF output indicates a larger increase in intense precipitation over time than the gridded product E-OBS.

For the short-duration extreme precipitation events (WRF 3-hourly), Figs. 5, 7(c,d) & 9 show that, regardless of the season, positive trends of extreme precipitation frequency and intensity dominate the European domain, which is consistent with Hosseinzadehtalaei et al. (2020), Cannon and Innocenti (2019) and Kendon et al. (2014). Moreover, Fig. 7(c,d) also shows the previously mentioned general positive trend. However, it also illustrates that the summer (JJA) has the strongest and most widespread positive trends with respect to other seasons. This is

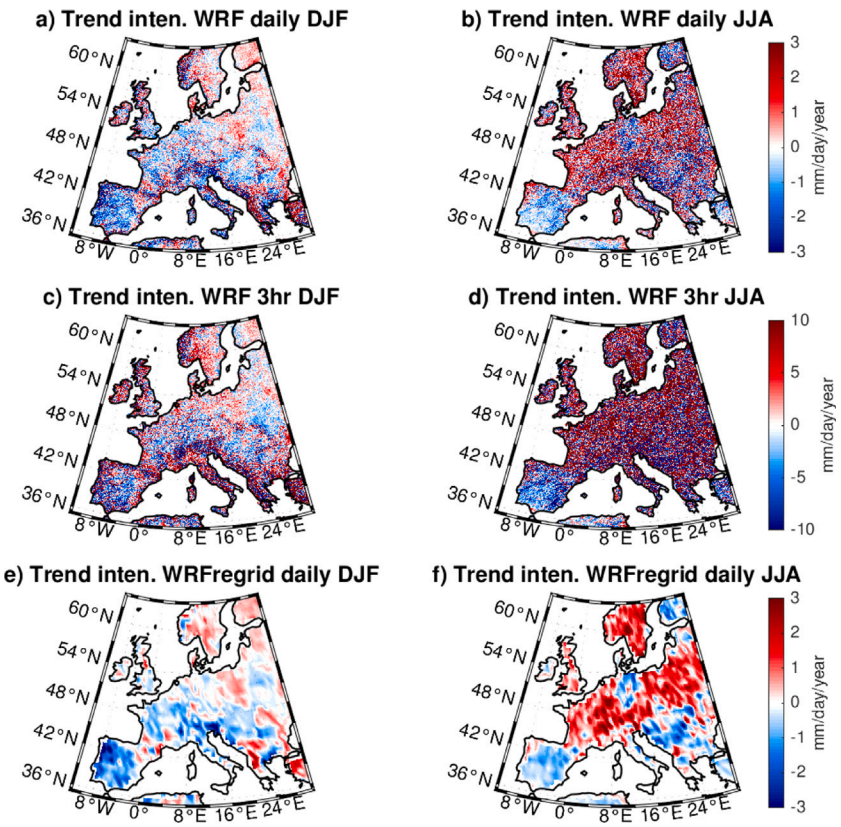

Fig. 7. Similar to Fig. 6, except for WRF daily data (1st row), WRF 3-hourly data (2nd row) and daily WRF data regridded to ERA-Interim resolution (3rd row).

discussed by Mishra et al. (2012) and Lenderink and van Meijgaard (2010), where it was shown that in summer the dependence of short-duration extreme precipitation on air temperature (Clausius–Clapeyron scaling) doubles with respect to winter.

Further investigations are carried out for the added value of the high resolution and the convection resolving dynamical downscaling. The analysis is repeated on WRF simulations after statistically regridding (upscaling) the data (see Section 2.2) to a resolution equivalent to that of ERA-Interim. Figs. 5, 7(e,f) show seasonal trends of extreme precipitation frequency and intensity for the regridded WRF simulations. The figures show that the trends of regridded WRF simulations in DJF do not change, and are consistent with those in E-OBS and ERA-Interim. In summer and transition seasons, regridded WRF still shows trends similar to these of the high resolution simulations. This is also shown in Fig. 9, where upscaling WRF from 4 km to a lower resolution does not dissipate the added value of the high resolution simulation, showing the same ratio as the high resolution data in all season.

We conclude that the difference in the statistical properties of extreme precipitation between ERA reanalysis and their WRF dynamical downscaling is not related to the size of the grid box over which averages are taken, but indeed it is related to the differences in the representation of small scale dynamics. We hypothesize that this is due to the convective parameterization used in the reanalysis, that provides different results from the mesoscale convection resolving WRF downscaling. We conclude that the dynamical downscaling at high resolution has a relevant impact on the statistics of extreme precipitation.

The 3-hourly ERA5 reanalysis shows inconsistent trends (summarized in Fig. 9) in some regions with respect to 3-hourly WRF and the previously mentioned literature regarding the sub-daily increase of extreme precipitation events as in Figs. 4, 6(g, h). ERA-Interim 6-hourly temporal resolution in Figure S7 shows that no improvements in the trends are becoming evident when considering a higher than daily temporal resolution. Overall, we conclude that a higher temporal resolution in the data obtained from a spatially low resolution model does not lead to significant improvements in the statistical properties of extreme precipitation.

4. Discussion and summary

In this study, different metrics of intense precipitation variability over the European region were analyzed using different data products. Gridded observations of daily precipitation (E-OBS) indicate that in the 30-year long study period and for all seasons except winter, more locations experienced an increase in extreme precipitation, both in term of frequency and of intensity, than those which recorded a decreasing trend. ERA-Interim reanalysis data, instead, showed an overall decrease in the intense precipitation in all seasons. Higher resolution ERA5 reanalysis showed results that better match those of E-OBS, but still reported an overall limited increase in the extreme precipitation especially during the summer season. The study then investigated the added-value of the dynamical downscaling of reanalysis with a convective-permitting model (WRF on a 4 km grid spacing). The patterns of extreme precipitation (95th percentile) look consistent in low and high resolution outputs, except for the detailed structure over the mountainous regions. The downscaling shows statistics of extreme precipitation that better match those computed on the gridded observation dataset E-OBS. Seasonal trends of frequency of occurrence and intensity of extreme precipitation were shown to be highly dependent on the temporal and spatial resolution for all seasons except for winter.

In different seasons, different factors are responsible for shaping extreme precipitation trends. In winter, the main driver of mean and extreme precipitation variability is the NAO (Hurrell, 1995; Casanueva et al., 2014). The overall consistency of all the data products during DJF is related to the fact that extreme winter precipitation in Europe is mainly controlled by the phase of the NAO, which is well d both in low and high resolution runs as it is a large scale process. During

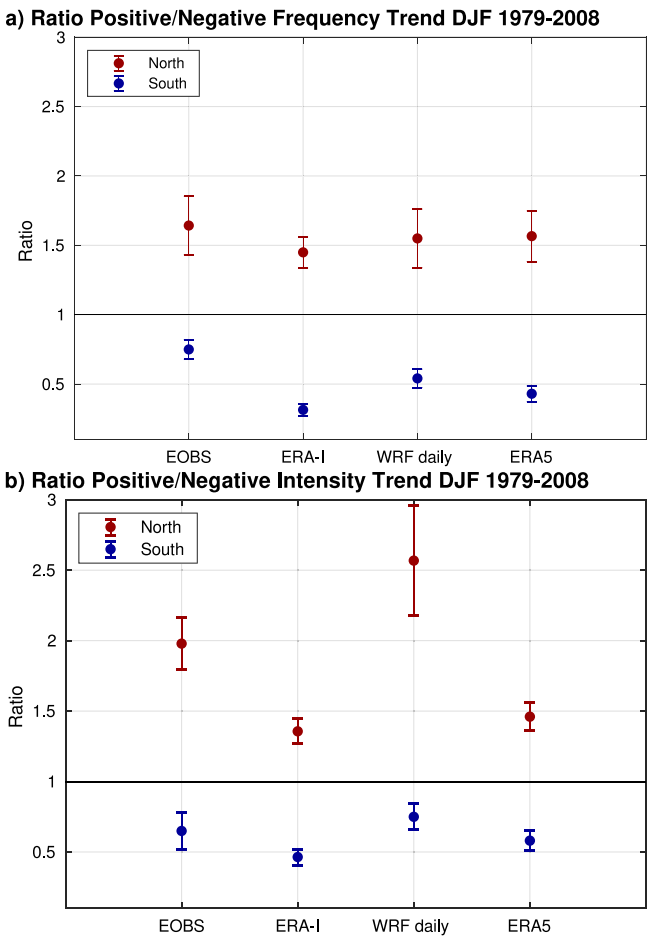

Fig. 8. Wintertime (DJF) ratio of positive to negative trends of extreme precipitation events frequency in E-OBS, ERA-Interim and ERA5 reanalysis, WRF daily data. Trend summation is calculated for northern and southern Europe. North: 49.1°N–63°N. South: 34°N–49°N. Error bars indicate the spread of the ratio by random sub-sampling within the domain.

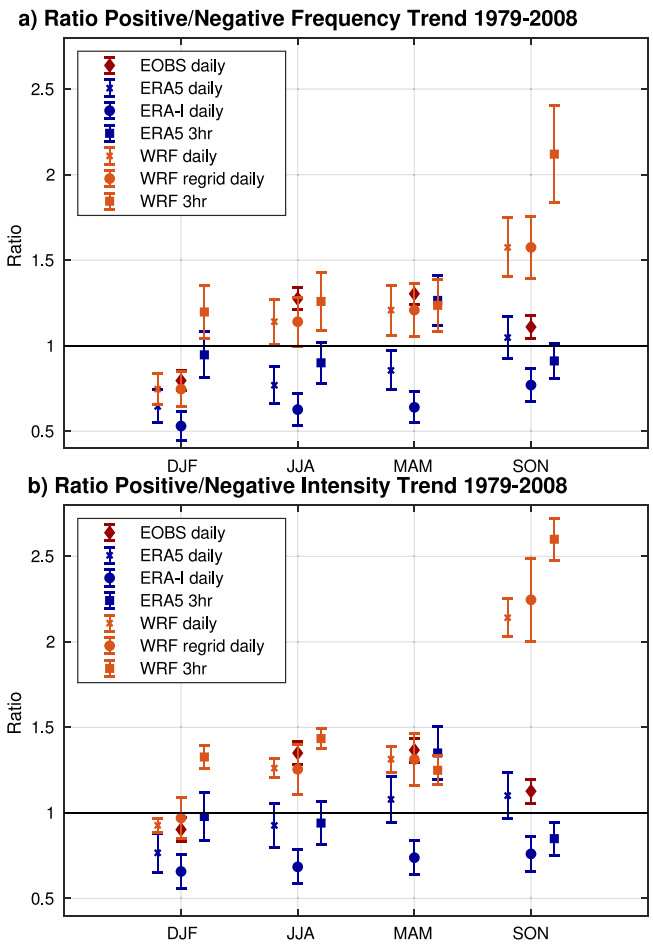

Fig. 9. Ratio of positive to negative trends of extreme precipitation events frequency in E-OBS, daily ERA-Interim reanalysis, daily and 3-hourly ERA5, WRF daily data at 4 km and regridded to ERA-Interim grid (WRF daily regrid), and WRF 3-hourly data, as shown in Figs. 4, 5, 6 & 7. Error bars indicate the spread of the ratio by random sub-sampling within the domain.

the 30 years of the analysis, NAO went from a period dominated by a negative phase to a period more dominated by a positive phase. The effect of this increase in NAO index is reflected in a reduction of extreme precipitation over the studied area. Investigation in a different period with a more stable NAO leads to different results for winter precipitation. It is still uncertain how future climate NAO will behave, as there is no observational-based evidence of a positive NAO trend forced by anthropogenic forcing. This remains an active area of research.

Another driver for European precipitation extremes in different seasons could be the Mediterranean Sea. It has been shown that the Mediterranean is a hot-spot for global warming (Giorgi, 2006) with increasing SSTs, which was particularly large in the period 2000–2012 (Rayner et al., 2003). Increased evaporation due to a warmer Mediterranean leads to enhanced moisture transport into Central Europe, possibly leading to more precipitation extremes there (Volosciuk et al., 2016). At the same time, precipitation can be reduced over the North Eastern Alps, due to a premature loss of moisture along the Adriatic Sea (Messmer et al., 2015). Dynamical changes under global warming scenarios, such as a poleward shift of cyclone tracks over Europe, might have the effect of decreasing the frequency of Vb cyclones (Messmer et al., 2020), further complicating the anticipation of future evolution of extreme precipitation.

CRediT authorship contribution statement

Mostafa E. Hamouda: Analyzed the data, Conceiving and designing the study, Interpreting the results, Writing - original draft. **Claudia Pasquero:** Conceiving and designing the study, Interpreting the results, Writing - original draft.

Declaration of competing interest

The authors declare that they have no known competing financial interests or personal relationships that could have appeared to influence the work reported in this paper.

Acknowledgments

M.E.H was supported by Cariplo Foundation, Italy, EXTRA project, and HPC-TRES grant number 2017-03. This article is an outcome of Progetto Dipartimenti di Eccellenza, funded by MIUR. We acknowledge CINECA HPC grant IsC65_CSIPAR and FAQC UniMiB grant.

Appendix A. Supplementary data

Supplementary material related to this article can be found online at https://doi.org/10.1016/j.wace.2021.100337.

References

Ban, Nikolina, Rajczak, Jan, Schmidli, Juerg, Schär, Christoph, 2020. Analysis of Alpine precipitation extremes using generalized extreme value theory in convection-resolving climate simulations. Clim. Dynam. 55.

Ban, Nikolina, Schmidli, Juerg, Schär, Christoph, 2015. Heavy precipitation in a changing climate: Does short-term summer precipitation increase faster? Geophys. Res. Lett. 42 (4), 1165–1172.

Bladé, I., Liebmann, B., Fortuny, D., Oldenborgh, G.J., 2011. Observed and simulated impacts of the summer NAO in Europe: implications for projected drying in the Mediterranean region. Clim. Dynam. 39, 709–727.

Buehler, Tania, Raible, Christoph C., Stocker, Thomas F., 2011. The relationship of winter season North Atlantic blocking frequencies to extreme cold or dry spells in the ERA-40. Tellus A 63 (2), 212–222.

Cannon, A.J., Innocenti, S., 2019. Projected intensification of sub-daily and daily rainfall extremes in convection-permitting climate model simulations over North America: implications for future intensity–duration–frequency curves. Nat. Hazards Earth Syst. Sci. 19 (2), 421–440.

Casanueva, A., Rodríguez-Puebla, C., Frías, M.D., González-Reviriego, N., 2014. Variability of extreme precipitation over Europe and its relationships with teleconnection patterns. Hydrol. Earth Syst. Sci. 18 (2), 709–725.

Cohen, Judah, Screen, James, Furtado, Jason, Barlow, Mathew, Whittleston, David, Coumou, Dim, Francis, Jennifer, Dethloff, Klaus, Entekhabi, Dara, Overland, James, Jones, Justin, 2014. Recent Arctic amplification and extreme mid-latitude weather. Nat. Geosci. 7, 627–637.

Cornes, Richard C., van der Schrier, Gerard, van den Besselaar, Else J.M., Jones, Philip D., 2018. An ensemble version of the E-OBS temperature and precipitation data sets. J. Geophys. Res.: Atmos. 123 (17), 9391–9409.

de Leeuw, J., Methven, J., Blackburn, M., 2015. Evaluation of ERA-interim reanalysis precipitation products using England and Wales observations. Q. J. R. Meteorol. Soc. 141 (688), 798–806.

Dee, D.P., Uppala, S.M., Simmons, A.J., Berrisford, P., Poli, P., Kobayashi, S., Andrae, U., Balmaseda, M.A., Balsamo, G., Bauer, P., Bechtold, P., Beljaars, A.C.M., van de Berg, L., Bidlot, J., Bormann, N., Delsol, C., Dragani, R., Fuentes, M., Geer, A.J., Haimberger, L., Healy, S.B., Hersbach, H., Hólm, E.V., Isaksen, L., Kållberg, P., Köhler, M., Matricardi, M., McNally, A.P., Monge-Sanz, B.M., Morcrette, J.-J., Park, B.-K., Peubey, C., de Rosnay, P., Tavolato, C., Thépaut, J.-N., Vitart, F., 2011. The ERA-Interim reanalysis: configuration and performance of the data assimilation system. Q. J. R. Meteorol. Soc. 137 (656), 553–597.

Dereczynski, Claudine, Chan Chou, Sin, Lyra, André, Sondermann, Marcely, Regoto, Pedro, Tavares, Priscila, Chagas, Diego, Gomes, Jorge Luís, Rodrigues, Daniela Carneiro, de los Milagros Skansi, María, 2020. Downscaling of climate extremes over South America – Part I: Model evaluation in the reference climate. Weather Clim. Extremes 29, 100273.

Deser, Clara, 2000. On the teleconnectivity of the "Arctic Oscillation". Geophys. Res. Lett. 27 (6), 779–782.

Fischer, Erich, Knutti, Reto, 2016. Observed heavy precipitation increase confirms theory and early models. Nature Clim. Change 6.

Folland, Chris K., Knight, Jeff, Linderholm, Hans W., Fereday, David, Ineson, Sarah, Hurrell, James W., 2009. The summer north atlantic oscillation: Past, present, and future. J. Clim. 22 (5), 1082–1103.

Frei, Christoph, Schär, Christoph, 1998. A precipitation climatology of the Alps from high-resolution rain-gauge observations. Int. J. Climatol. 18 (8), 873–900.

Giorgi, F., 2006. Climate change hot-spots. Geophys. Res. Lett. 33 (8).

Giorgi, Filippo, Torma, Csaba, Coppola, Erika, Ban, Nikolina, Schär, Christoph, Somot, Samuel, 2016. Enhanced summer convective rainfall at Alpine high elevations in response to climate warming. Nat. Geosci. 9.

Goodess, C.M., Jones, P.D., 2002. Links between circulation and changes in the characteristics of Iberian rainfall. Int. J. Climatol. 22 (13), 1593–1615.

Guérémy, J.-F., Laanaia, N., Céron, J.-P., 2012. Seasonal forecast of French Mediterranean heavy precipitating events linked to weather regimes. Nat. Hazards Earth Syst. Sci. 12 (7), 2389–2398.

Hersbach, Hans, Bell, Bill, Berrisford, Paul, Hirahara, Shoji, Horányi, András, Muñoz-Sabater, Joaquín, Nicolas, Julien, Peubey, Carole, Radu, Raluca, Schepers, Dinand, Simmons, Adrian, Soci, Cornel, Abdalla, Saleh, Abellan, Xavier, Balsamo, Gianpaolo, Bechtold, Peter, Biavati, Gionata, Bidlot, Jean, Bonavita, Massimo, De Chiara, Giovanna, Dahlgren, Per, Dee, Dick, Diamantakis, Michail, Dragani, Rossana, Flemming, Johannes, Forbes, Richard, Fuentes, Manuel, Geer, Alan, Haimberger, Leo, Healy, Sean, Hogan, Robin J., Hólm, Elías, Janisková, Marta, Keeley, Sarah, Laloyaux, Patrick, Lopez, Philippe, Lupu, Cristina, Radnoti, Gabor, de Rosnay, Patricia, Rozum, Iryna, Vamborg, Freja, Villaume, Sebastien, Thépaut, Jean-Noël, 2020. The ERA5 global reanalysis. Q. J. R. Meteorol. Soc. 146 (730), 1999–2049.

Hodnebrog, Ø, Marelle, L, Alterskjær, K, Wood, R.R., Ludwig, R, Fischer, E.M., Richardson, T.B., Forster, P.M., Sillmann, J, Myhre, G, 2019. Intensification of summer precipitation with shorter time-scales in Europe. Environ. Res. Lett. 14 (12), 124050.

Hofstätter, Michael, Chimani, Barbara, 2012. Van Bebber's cyclone tracks at 700 hPa in the Eastern Alps for 1961–2002 and their comparison to Circulation Type Classifications. Meteorol. Z. 21, 459–473.

Hofstra, Nynke, Haylock, Malcolm, New, Mark, Jones, P., 2009. Testing E-OBS European high-resolution gridded data set of daily precipitation and surface temperature. J. Geophys. Res. D 114, 11, D21101.

Hosseinzadehtalaei, Parisa, Tabari, Hossein, Willems, Patrick, 2020. Climate change impact on short-duration extreme precipitation and intensity–duration–frequency curves over europe. J. Hydrol. 590, 125249.

Huang, Danqing, Yan, Peiwen, Zhu, Jian, Zhang, Yaocun, Kuang, Xueyuan, Cheng, Jing, 2017. Uncertainty of global summer precipitation in the CMIP5 models: a comparison between high-resolution and low-resolution models. Theor. Appl. Climatol.

Hurrell, James W., 1995. Decadal trends in the north atlantic oscillation: Regional temperatures and precipitation. Science 269 (5224), 676–679.

Hurrell, J.W, Kushnir, Yochanan, Ottersen, Geir, Visbeck, Martin, 2003. The north atlantic oscillation: Climatic significance and environmental impact. Geophys. Monogr. Ser. 134.

Husak, Gregory J., Michaelsen, Joel, Funk, Chris, 2007. Use of the gamma distribution to represent monthly rainfall in Africa for drought monitoring applications. Int. J. Climatol. 27 (7), 935–944.

IPCC, 2013. Summary for policymakers. In: Stocker, T.F., Qin, D., Plattner, G.-K., Tignor, M., Allen, S.K., Boschung, J., Nauels, A., Xia, Y., Bex, V., Midgley, P.M. (Eds.), Climate Change 2013: The Physical Science Basis. Contribution of Working Group I to the Fifth Assessment Report of the Intergovernmental Panel on Climate Change. Cambridge University Press, Cambridge, United Kingdom and New York, NY, USA, pp. 1–30.

Isotta, Francesco A., Frei, Christoph, Weilguni, Viktor, Perčec Tadić, Melita, Lassègues, Pierre, Rudolf, Bruno, Pavan, Valentina, Cacciamani, Carlo, Antolini, Gabriele, Ratto, Sara M., Munari, Michela, Micheletti, Stefano, Bonati, Veronica, Lussana, Cristian, Ronchi, Christian, Panettieri, Elvio, Marigo, Gianni, Vertačnik, Gregor, 2014. The climate of daily precipitation in the Alps: development and analysis of a high-resolution grid dataset from pan-Alpine rain-gauge data. Int. J. Climatol. 34 (5), 1657–1675.

James, P., Stohl, A., Spichtinger, N., Eckhardt, S., Forster, C., 2004. Climatological aspects of the extreme European rainfall of August 2002 and a trajectory method for estimating the associated evaporative source regions. Nat. Hazards Earth Syst. Sci. 4 (5/6), 733–746.

Jones, Philip W., 1999. First- and second-order conservative remapping schemes for grids in spherical coordinates. Mon. Weather Rev. 127 (9), 2204–2210.

Kendon, Elizabeth, Roberts, Nigel, Fowler, Hayley, Roberts, Malcolm, Chan, Steven, Senior, Catherine, 2014. Heavier summer downpours with climate change revealed by weather forecast resolution model. Nature Clim. Change 4, 570–576.

Krug, Amelie, Pothapakula, Praveen Kumar, Primo, Cristina, Ahrens, Bodo, 2021. Heavy Vb–cyclone precipitation: a transfer entropy application showcase. Meteorol. Z.

Lenderink, Geert, van Meijgaard, Erik, 2010. Linking increases in hourly precipitation extremes to atmospheric temperature and moisture changes. Environ. Res. Lett. 5 (2), 025208.

Leutwyler, David, Lüthi, Daniel, Ban, Nikolina, Fuhrer, Oliver, Schär, Christoph, 2017. Evaluation of the convection-resolving climate modeling approach on continental scales. J. Geophys. Res.: Atmos. 122 (10), 5237–5258.

Messmer, Martina, Gómez-Navarro, Juan, Raible, Christoph, 2015. Climatology of Vb-cyclones, physical mechanisms and their impact on extreme precipitation over Central Europe. Earth Syst. Dyn. 6, 541–553.

Messmer, Martina, Gomez-Navarro, Juan, Raible, Christoph, 2016. Sensitivity experiments on the response of Vb cyclones to ocean temperature and soil moisture changes.

Messmer, Martina, Raible, Christoph C., Gomez-Navarro, Juan Jose, 2020. Impact of climate change on the climatology of Vb cyclones. Tellus A 72 (1), 1–18.

Mishra, Vimal, Wallace, John M., Lettenmaier, Dennis P., 2012. Relationship between hourly extreme precipitation and local air temperature in the United States. Geophys. Res. Lett. 39 (16).

Myhre, Gunnar, Alterskjær, Kari, Stjern, Camilla, Hodnebrog, Øivind, Marelle, Louis, Samset, B., Sillmann, Jana, Schaller, Nathalie, Fischer, Erich, Schulz, M., Stohl, Andreas, 2019. Frequency of extreme precipitation increases extensively with event rareness under global warming. Sci. Rep. 9, 16063.

North, Gerald, Bell, Thomas, Cahalan, Robert, Moeng, Fanthune, 1982. Sampling errors in the estimation of empirical orthogonal functions. Mon. Weather Rev. 110.

Papalexiou, Simon Michael, Montanari, Alberto, 2019. Global and regional increase of precipitation extremes under global warming. Water Resour. Res. 55 (6), 4901–4914.

Pieri, Alexandre B., von Hardenberg, Jost, Parodi, Antonio, Provenzale, Antonello, 2015. Sensitivity of precipitation statistics to resolution, microphysics, and convective parameterization: A case study with the high-resolution WRF climate model over Europe. J. Hydrometeorol. 16 (4), 1857–1872.

Pinto, Joaquim G., Raible, Christoph C., 2012. Past and recent changes in the North Atlantic Oscillation. WIREs Clim. Change 3 (1), 79–90.

Raible, C.C., 2007. On the relation between extremes of midlatitude cyclones and the atmospheric circulation using ERA40. Geophys. Res. Lett. 34 (7).

Raible, Christoph Cornelius, Ziv, Baruch, Saaroni, Hadas, Wild, Martin, 2009. Winter synoptic-scale variability over the Mediterranean Basin under future climate conditions as simulated by the ECHAM5. Clim. Dynam. 35.

Rayner, N.A., Parker, D.E., Horton, E.B., Folland, C.K., Alexander, L.V., Rowell, D.P., Kent, E.C., Kaplan, A., 2003. Global analyses of sea surface temperature, sea ice, and night marine air temperature since the late nineteenth century. J. Geophys. Res.: Atmos. 108 (D14).

Santos, Mónica, Fonseca, Andre, Fragoso, Marcelo, Santos, João, 2018. Recent and future changes of precipitation extremes in mainland Portugal. Theor. Appl. Climatol.

Scaife, Adam, Folland, Chris, Alexander, Lisa, Moberg, A., Knight, J.R., 2008. European climate extremes and the North Atlantic Oscillation. J. Clim. 21, 72–83.

Schär, Christoph, Ban, Nikolina, Fischer, Erich, Rajczak, Jan, Schmidli, Juerg, Frei, Christoph, Giorgi, Filippo, Karl, T.R., Kendon, Elizabeth, Tank, Albert, O'Gorman, Paul, Sillmann, Jana, Zhang, Xuebin, Zwiers, Francis, 2016. Percentile indices for assessing changes in heavy precipitation events. Clim. Change 137.

Seneviratne, Sonia, Nicholls, Neville, Easterling, D., Goodess, C., Kanae, S., Kossin, J., Luo, Yuwei, Marengo, Jose, Mcinnes, Kathleen, Rahimi, Mohammad, Reichstein, Markus, Sorteberg, Asgeir, Vera, Carolina, Zhang, Xuebin, 2012. Changes in climate extremes and their impacts on the natural physical environment: An overview of the IPCC SREX report. p. 12566.

Sillmann, Jana, Croci-Maspoli, Mischa, 2009. Present and future atmospheric blocking and its impact on European mean and extreme climate. Geophys. Res. Lett. 36 (10).

Skok, Gregor, Žagar, Nedjeljka, Honzak, Luka, Žabkar, Rahela, Rakovec, Joze, Ceglar, Andrej, 2015. Precipitation intercomparison of a set of satellite- and raingauge-derived datasets, ERA interim reanalysis, and a single WRF regional climate simulation over Europe and the North Atlantic. Theor. Appl. Climatol. 123.

Stohl, Andreas, James, Paul, 2005. A Lagrangian analysis of the atmospheric branch of the global water cycle. Part II: Moisture transports between earth's ocean basins and river catchments. J. Hydrometeorol. 6 (6), 961–984.

Thompson, Gregory, Rasmussen, Roy, Manning, Kevin, 2004. Explicit forecasts of winter precipitation using an improved bulk microphysics scheme. Part I: Description and sensitivity analysis. Mon. Weather Rev. 132, 519–542.

Thompson, David W.J., Wallace, John M., 1998. The arctic oscillation signature in the wintertime geopotential height and temperature fields. Geophys. Res. Lett. 25 (9), 1297–1300.

Totz, Sonja, Tziperman, Eli, Coumou, Dim, Pfeiffer, Karl, Cohen, Judah, 2017. Winter precipitation forecast in the European and mediterranean regions using cluster analysis. Geophys. Res. Lett. 44 (24), 12,418–12,426.

Trenberth, Kevin, 2011. Changes in precipitation with climate change. Clim. Res. 47, 123–138.

Trenberth, K.E., Josey, Simon, 2007. Observations: surface and atmospheric climate change.

van Bebber, W., 1891. Die Zugstrassen der barometrischen Minima nach den Bahnenkarten der Deutschen Seewarte fuer den Zeitraum 1875–1890. Meteorol. Z. 8, 361–366.

Volosciuk, Claudia, Maraun, Douglas, Semenov, V., Tilinina, Natalia, Gulev, Sergey, Latif, M., 2016. Rising mediterranean sea surface temperatures amplify extreme summer precipitation in central Europe. Sci. Rep. 6, 32450.

Walker, G.T., Bliss, E.W., 1932. World weather. V. Mem. Roy. Meteor. Soc. 4, 53–84.

Wang, Xiaolan L., Swail, Val R., Zwiers, Francis W., 2006. Climatology and changes of extratropical cyclone activity: Comparison of ERA-40 with NCEP–NCAR reanalysis for 1958–2001. J. Clim. 19 (13), 3145–3166.

Zolina, Olga, Simmer, Clemens, Belyaev, Konstantin, Kapala, Alice, Gulev, Sergey, 2009. Improving estimates of heavy and extreme precipitation using daily records from European rain gauges. J. Hydrometeorol. 10.

Zolina, Olga, Simmer, Clemens, Kapala, Alice, Bachner, Susanne, Gulev, Sergey, Maechel, Hermann, 2008. Seasonally dependent changes of precipitation extremes over Germany since 1950 from a very dense observational network. J. Geophys. Res.: Atmos. 113 (D6).

Zolina, Olga, Simmer, Clemens, Kapala, Alice, Gulev, Sergey, 2005. On the robustness of the estimates of centennial-scale variability in heavy precipitation from station data over Europe. Geophys. Res. Lett. 32.